



Original

Effect of oxygen addition on the formation of anatase TiO₂ nano-coatings obtained by spray pyrolysis technique

Zineb Benzait^{a,b,*}

Demet Tatar^a

Mehmet Ertuğrul^a

^aNanoscience and Nanoengineering Department, Atatürk University, Erzurum 2540, Turkey

^bNanoscience and Nanoengineering Department, Istanbul Technical University, Istanbul 34469, Turkey

Abstract: High-quality anatase phased titanium dioxide thin films were prepared in this work using an easy, simple and cost-effective method. Normal, partially and highly oxygen-enriched atmospheres were provided during the spray pyrolysis deposition of titania in order to study the oxygen effect on the structure and morphology of the films prepared. High crystalline anatase nano-coatings stable at high temperature (700°C) could be obtained through the delaying of anatase-to-rutile transformation due to the filling of oxygen vacancies by the oxygen added to the spraying atmosphere. These nano-coatings constitute promising materials for different applications such as hydroxyapatite coated metal implanting, rechargeable lithium ion batteries fabrication, gas sensing and photocatalytic applications.

Keywords: Titanium Dioxide, Anatase, Nano-coatings, Thin Films, Spray Pyrolysis Technique.

1. INTRODUCTION

Titanium dioxide, one of the most extensively investigated semiconductor oxides, finds extensive applications in the area of solar cells (El Kass et al., 2017; Giordano et al., 2016), photocatalysts (Singh et al., 2017), gas sensors (Park, Kim, Rana, Jamwal, & Katoch, 2017), water-splitting (Ziegler et al., 2016), cancer therapy (Na & Park, 2016), and self-cleaning materials (Vodišek, Ramanujachary, Brezová, & Lavrenčič Štangar, 2017; Chen & Mao, 2007).

TiO₂ is also considered as a promising material for the fabrication of safe anodes of rechargeable lithium ion batteries (Bai et al., 2016; Li et al., 2012). Among existing

TiO₂ nanostructures (anatase, rutile, brookite), anatase presents the most interesting electrochemical properties (Deng, Kim, Lee, & Cho, 2009); its good stability, low volume expansion (3–4%), high operating voltage (1.5–1.8 V vs Li/Li⁺) and low cost make it a great potential alternative material to graphite based anodes (Li et al., 2015). Furthermore, anatase TiO₂ possesses the best photocatalytic activity because of its large band gap (3.2 eV) and strong oxidizing power (Lv, Chen, Liu, Wang, & Meng, 2015a; Periyat, Naufal, & Ullattil, 2016) which make it highly useful in photocatalytic applications.

High crystalline anatase TiO₂ has also been reported to improve the osteogenic activity and enhance the hydroxyapatite (HA) formation on metallic implants due to lattice match and superposition of hydrogen-bonding groups in anatase crystals comparing to rutile crystals (Lv, Li, Xie, Cao, & Zheng, 2017; Uchida, Kim, Kokubo,

* Corresponding author.

E-mail address: zineb@itu.edu.tr (Zineb Benzait).

Fujibayashi, & Nakamura, 2003; Xia, Lindahl, Lausmaa, & Engqvist, 2011).

Although high thermal treatment improves the crystallinity of TiO_2 , it leads to undesirable anatase–rutile phase transformation which occurs generally below 600°C (Pillai et al., 2007). Various attempts have been made to improve the crystallinity of anatase TiO_2 while inhibiting its transformation to rutile such as metal or/and nonmetal doping, surface modification with metal oxides (i.e., Al_2O_3 , NiO, and ZnO) (Lv, Chen, Liu, Wang, & Meng, 2015b). However, the formation of secondary impurities (e.g. Al_2TiO_5 , NiTiO_3 , $\text{CeTi}_4\text{O}_{24}$, $\text{Ce}_2\text{Ti}_2\text{O}_7$, etc.) at high-temperature and the consequent decrease in photocatalytic activity make this technique disadvantageous (Lv, Yu, Huang, Liu, & Feng, 2009; Periyat et al., 2016; Pillai et al., 2007). Therefore, it is necessary to develop an effective method for the synthesis of stable anatase phased nanostructures without having such major drawbacks. In this article, we report an easy and economical route to prepare TiO_2 nano-coatings with delaying the anatase-to-rutile transformation by adding oxygen to the atmosphere of spray pyrolysis deposition.

Some recent works have reported the preparation of TiO_2 thin films using several methods such as atomic layer deposition (Piercy, Leng, & Losego, 2017), chemical vapor deposition (Rahim, Sahdan, Bakri, Yunus, & Lias, 2016), pulsed laser deposition (Wang et al., 2017) and sputtering (Ben Jemaa, Chaabouni, & Abaab, 2017; Singh et al., 2017). Although they produce high-quality semiconductor thin films, these systems involve very high vacuum or/and temperature, are not suitable for large-area substrates, have low throughput and complex operating conditions, furthermore, they are high-cost equipment and production techniques (Dominguez & Orduña-Díaz, 2017; Jameel, 2015). By contrast, solution-based deposition processes offer cost-effectiveness, simplicity, compatibility with large-area substrates, moreover, possibility of scaling up to industrial level (Song, 2016; You, 2015). Among these solution-process techniques, sol-gel route (Aminirastabi, Weng, Xiong, Ji, & Xue, 2017; Parveen, Mahmood-ul-Hassan, Khalid, Riaz, & Naseem, 2017), chemical bath deposition (Dhandayuthapani, Sivakumar, & Ilangoan, 2016; Govindasamy, Murugasen, Sagadevan, 2016) and spray pyrolysis technique (Chandrashekhara, Angadi, Ravikiran, et al., 2016; Chandrashekhara, Angadi, Shashidhar, Murthy, & Poornima, 2016) have been recently used in TiO_2 thin film production.

In the present work, spray pyrolysis technique (SPT) has been chosen due to the simplicity of its apparatus and operation, its ability to produce low-cost and high crystalline oxide layers with high quality adherence and uniform thickness, its ability of coating large and complex geometries, in addition to the possibility of scaling it up for industrial applications (Chourashiya, 2013; Filipovic et al., 2013; Shinde, 2012).

2. EXPERIMENTAL METHODS AND MATERIALS

Specimens of stainless steel with dimensions of ($1\text{cm} \times 1\text{cm} \times 0,127\text{cm}$), used as substrates, were ultrasonically cleaned in methanol, acetone and deionized water for 10 minutes each time then dried. Precursor solution containing 6 vol. % titanium (IV) isopropoxide (TTIP) and ethanol, provided by *Sigma-Aldrich*, was prepared. Acetylacetone (AcAc) provided from *Merck Schuchardt OHG* was added as a stabilizer in a molar ratio of TTIP:AcAc = 1:2.

To synthesize TiO_2 nanostructured thin films, a home-made spray pyrolysis equipment illustrated in the next schematic diagram was used (Figure 1): a pneumatic nozzle sprays fine droplets of the precursor solution using compressed air as a carrier gas, while a rotating plate carries the substrate specimens is heated by halogen lamps controlled using a temperature regulator system.

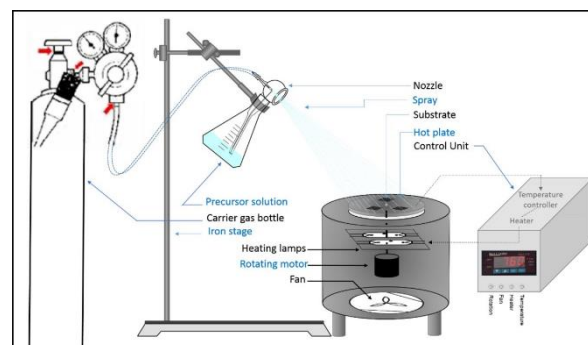


Fig. 1. Schematic diagram of the home-made SPT equipment used.

First of all, in order to find the optimum SPT process conditions, the substrate temperature was varied from 320 to 420°C when keeping the other parameters constant (solution concentration (6%), spraying solution quantity (100 ml), distance (35 cm)). Secondly, the experiments were performed at the optimum temperature, with and

without an additional flow of oxygen directed to the substrates to study the O₂ addition effect. It is worth noting that a post-heat treatment of all the prepared films was carried out at 700°C for one hour in normal atmosphere using a 3 zone-tube furnace (PZE 12/50/500, Protherm Furnace, Turkey).

The evaluation of crystallinity and composition of the prepared TiO₂ thin films was carried out using an X-Ray diffractometer (Cu K α radiation ($\lambda=0.154$ nm), GNR APD 2000 PRO, Ataturk University) ($\lambda=0.154$ nm). Morphology and cross-section of the coatings were examined by a high-resolution field emission scanning electron microscope (Quanta 450 FEG FE-SEM; Erzincan University). Elemental analysis was carried out by energy dispersive X-ray spectroscopy (EDS) detector connected with FE-SEM.

3. RESULTS AND DISCUSSIONS

For the purpose of optimizing the most important SPT parameter, the effect of substrate temperature was first studied. Figure 2 illustrates the XRD patterns of films deposited under O₂-enriched atmosphere at different temperatures. According to the standard JCPDS card no: 71-1166, in all the films except that deposited at 320°C, TiO₂ anatase crystalline phase was formed and its main peak at 25,3°, corresponding to (101) diffraction plane, was clearly detected. Intensities of (101) peak and the other minor peaks increased progressively with the substrate temperature which illustrates the improvement of films crystallinity. These results can be explained by elucidating the different processes that take place by virtue of temperature (Filipovic, et al., 2013; Nakaruk & Sorrell, 2010):

- For films deposited at 320°C which is considered low, the thermal gradient was not sufficient to miniaturize the droplets, which approached the substrate in their big form and precipitated in its surface as an amorphous salt (Ti[OH]₄) (Process A).
- For the films deposited at 350° and 380°C, the droplets were greatly evaporated, and the generated aerosols precipitated before arriving at the surface, then the formed precipitates oxidized partially when arriving at the substrate surface (Process B). Consequently, 350°-380°C temperatures are considered intermediate and hence not suitable to establish a perfect deposition process.

- For the films deposited at 400° and most importantly at 420°C, the thermal gradient was adequate to diminish the size of the droplets, to evaporate them extensively, and to cause an early precipitation of their aerosols. The obtained precipitates sublimed immediately just before attending the substrate. When this sublimate came into collision with the surface, it subsequently oxidized then got adsorbed chemically (CVD-like process, process C in Figure 3). In conclusion, substrate temperature nearly equal to 420°C is necessary to carry out the most desired CVD-like mechanism which provides the synthesis of well crystallized TiO₂ films.

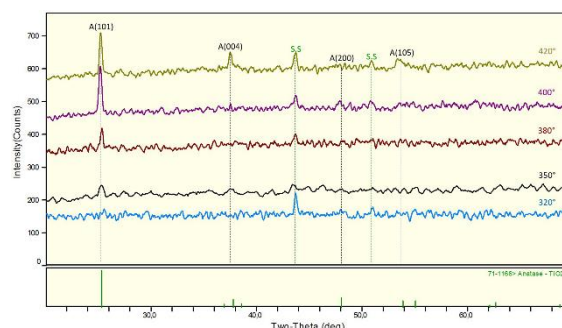


Fig. 2. XRD patterns of TiO₂ thin films deposited at different temperatures, after annealing at 700°C.

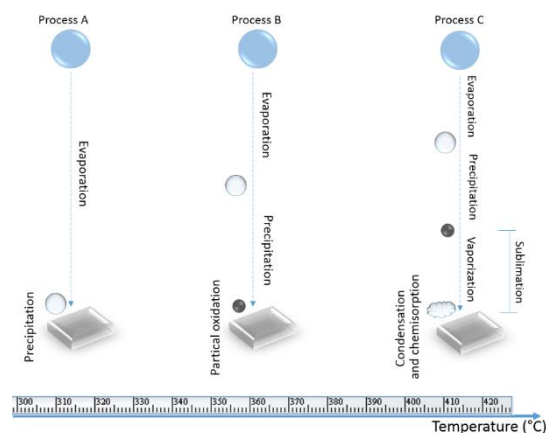


Fig. 3. Effect of substrate temperature on SPT processes.

After determining the optimum temperature, new experiments were carried-out at 420 °C to study the effect of oxygen addition to the spray environment on the titania films crystallinity and morphology.

Figure 4 of the obtained XRD patterns demonstrates that oxygen has a great influence in the films crystalline phase: Films deposited under a high oxygen pressure exhibit XRD peaks correspond to a pure TiO₂ anatase phase according to the Standard JCPDS card no:71-1166. In contrast, films obtained without adding an oxygen flow in the SPT process exhibit TiO₂ rutile peaks as it is given by JCPDS card no:76-0649. Whereas coatings deposited under low-pressure O₂-enriched atmosphere exhibit peaks of both phases with a remarked drop in their intensities which means that these coatings are composed of a mixture of anatase and rutile.

To understand the phenomena behind these results, as-deposited films were also characterized. All the as-deposited films consist of pure anatase phase whatever is the degree of oxygen-enrichment (Figure 5). Since the surface Gibbs free energy of anatase is lower than that of rutile phase, TiO₂ initially prefers to nucleate into anatase phase rather than into rutile phase (Choudhury & Choudhury, 2013).

Per contra, after being annealed at 700°C, coatings synthesized in normal atmosphere exhibit new rutile phase (Figure 4) which signifies that a phase transformation occurred due to heat treatment. Some other writers reported similar results for films obtained without adding oxygen (Castañeda et al., 2003; Nakaruk, Ragazzon, & Sorrell, 2010; Oja, Mere, Krunk, Solterbeck, & Es-Souni, 2004).

Theoretically, pure anatase begins to transform to rutile in air below 600°C, however, it may vary with different factors such as the number of oxygen vacancies which cause positive strain in anatase lattice. These crystalline defects can be removed by heat treatment which provides the activation energy necessary to relax the lattice and rearrange it to the rutile state (Choudhury & Choudhury, 2013; Hanaor & Sorrell, 2011). Filling those vacancies by O₂ molecules can partially or completely inhibit the transformation to rutile, which is the case of our films deposited under low or high pressure O₂-enriched atmosphere. The above explanation of the obtained results can be confirmed by two previous studies:

- Thin films of Co-TiO₂ were deposited using pulsed laser deposition (PLD) technique at various oxygen partial pressures. At higher oxygen partial pressure, the dominant phase was anatase inhibited to be transformed to rutile (Ali, Rumaiz, Ozbay, Nowak, & Ismat Shah, 2009).

- High-temperature stable anatase phased nanocrystalline titania was synthesized by a reaction of amorphous titanium dioxide with hydrogen peroxide (H₂O₂ - TiO₂) followed by a calcination process. In this route, in-situ generation of oxygen through thermal decomposition of peroxo-titania complex prevented the phase transformation of the produced nano-powder from anatase to rutile (Etacheri, Seery, Hinder, & Pillai, 2011).

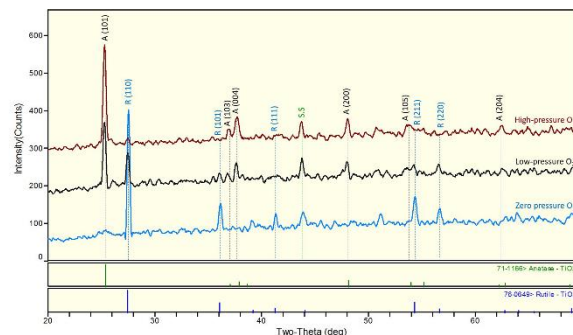


Fig. 4. XRD patterns of TiO₂ films obtained with high-pressure, low pressure and zero pressure O₂ addition to the spraying atmosphere, after annealing at 700°C.

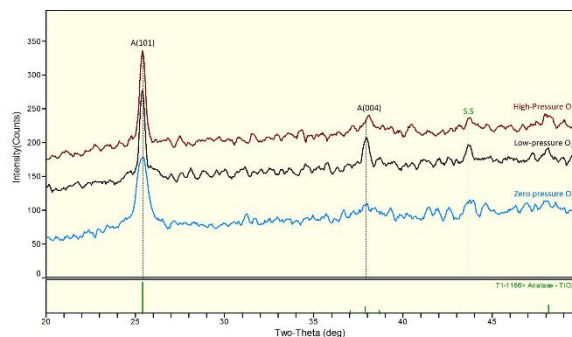


Fig. 5. XRD patterns of the as-deposited TiO₂ films obtained with high-pressure, low pressure and zero pressure O₂ addition to the spraying atmosphere.

In our study, anatase phase was conserved and prevented from being transformed to rutile because the low or high amount of oxygen provided in spraying process was absorbed, and oxygen vacancies were -respectively- partially or completely filled.

To the best of our knowledge, there are no systematic studies that reported the synthesis of high-temperature stable anatase TiO₂ thin film by spray pyrolysis technique without using any dopants. Thus, we report in this work a new, easy and economical route to synthesize stable and high crystalline anatase nano-coating deposited under O₂-enriched atmosphere by SPT.

Average sizes of the obtained thin films crystallites were determined using the famous Scherrer's formula:

$$D = \frac{K \lambda}{\beta \cos \theta} \quad (1)$$

D is the mean grain size of nanoparticles, $K=0.9$, the diffractometer used is with $\text{CuK}\alpha$ radiation thus the wavelength $\lambda=1,5406\text{\AA}$, θ is Bragg's angle and β is the full width at half of the peak maximum (FWHM) correspond to the main peak A(101) for anatase phase and R(110) peak for rutile phase.

The amount of anatase phase in bi-phased films was determined using Spurr equation:

$$F_A = \frac{1}{1 + 1,26\left(\frac{I_r}{I_a}\right)} \quad (2)$$

F_A is the anatase amount in the anatase-rutile mixture, I_a and I_r are the intensities of anatase and rutile main peak, ie (101) and (110) respectively.

Qualitative assessment reveals that the film deposited under high-pressure O_2 -enriched atmosphere is composed of anatase crystallites with ~ 33 nm in size. Oppositely, the film deposited under normal atmosphere consists of rutile phase which its grains size is about 52 nm. This film was first composed of anatase, however, after being annealed at 700°C it was completely transformed to rutile with bigger crystallite size. In contrast, the film deposited under low-pressure O_2 -enriched atmosphere shows a mixture of 56% anatase and 44% rutile crystallites with sizes of 42 nm and 45 nm respectively. In this film, a partial transformation of anatase to rutile occurred and was

accompanied by grain growth, this resulted in a nano-coating constituted of large rutile grains and small anatase grains. These calculations were confirmed by scanning electron microscopy images reported in Figure 6.

Figure 6a shows the morphology of the film deposited in an environment rich in O_2 . This film is fully dense, composed of aggregates which are primary small particles. In contrast, the film deposited without enriching the deposition atmosphere with oxygen (Figure 6c) consists largely of square-based pyramidal individual grains with narrow size distribution. These grains size is relatively large comparing to those of the film shown in Figure 6a.

Deposition of Titania in a partially O_2 -enriched atmosphere results in the film presented in Figure 6b. The structure of this film exhibits a mixture of individual grains and agglomerated small particles. These results confirm those obtained by XRD: rutile grains which constitute the film shown in Figure 6c are bigger than the anatase ones which constitute the film shown in Figure 6a, and the film illustrated in Figure 6b is a mixture of both phases with near grain sizes according to SEM morphology, exactly as it was concluded from XRD patterns.

The cross-section of a representative TiO_2 thin film is presented in Figure 7. It is clearly observed that the nano-coatings prepared in this work using SPT method are very thin, continuous and smooth with a uniform thickness of approximately 414 nm.

The EDS patterns of the previous films (Figure 8) confirm again the effect of oxygen addition to the deposition environment. O_2 addition allows the formation of interstitial oxygen in anatase TiO_2 thin films. On the other hand, the absence of oxygen leads to thin films with lower composition of O_2 ($\text{Ti}/\text{O}=1,54$ w/w, $\text{TiO}_{1,94}$ which comply with the rutile formula TiO_{2-x}).

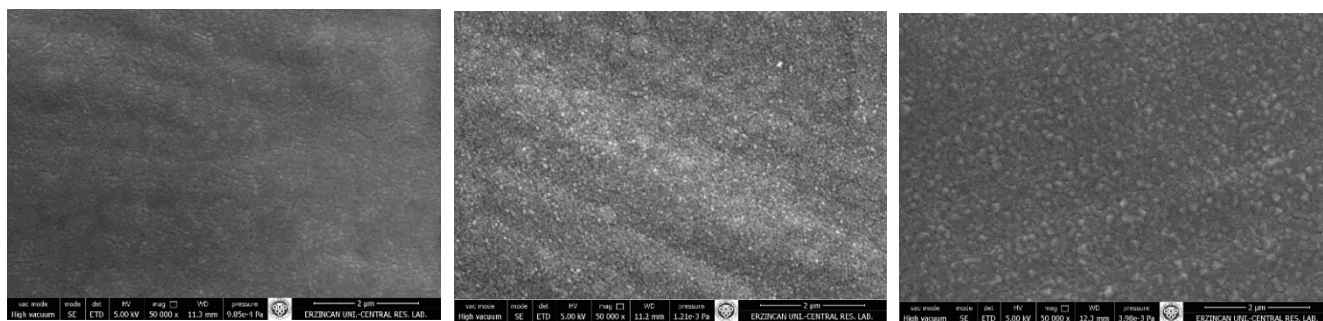


Fig. 6. Representative FE-SEM images of the films deposited at 420°C under (a) under high-pressure O_2 -enriched atmosphere, (b) low-pressure O_2 -enriched atmosphere, and (c) normal atmosphere.

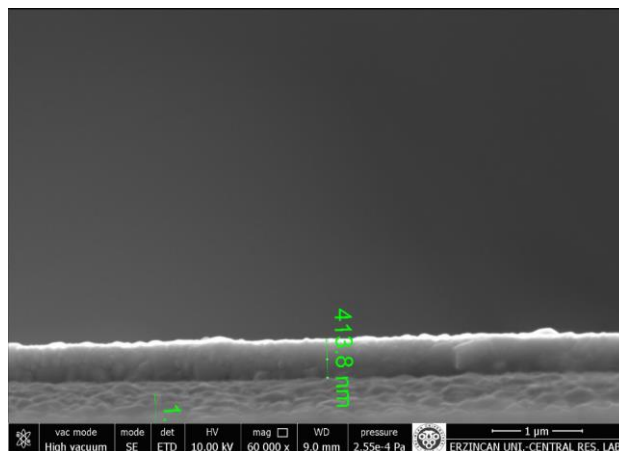


Fig. 7. Cross-section of a typical prepared TiO_2 nano-coating.

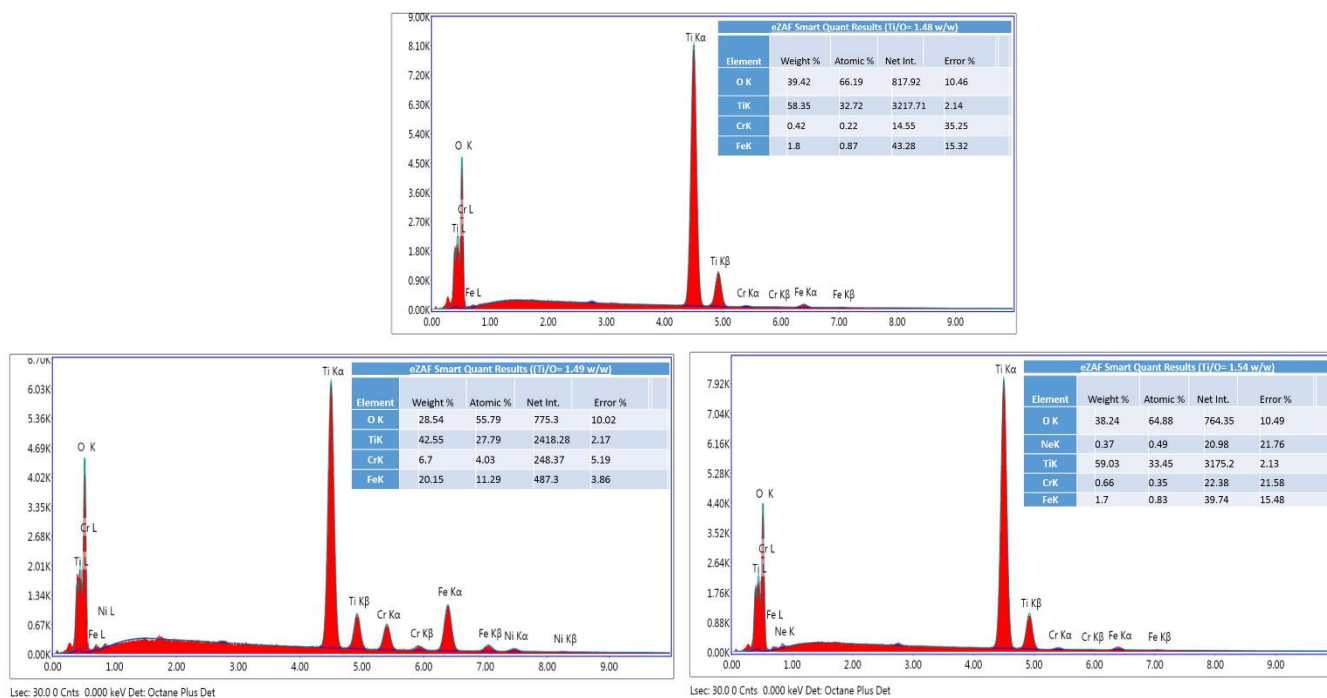


Fig. 8. EDS of the films deposited under (a) under high-pressure O_2 -enriched atmosphere, (b) low-pressure O_2 -enriched atmosphere, and (c) normal atmosphere.

4. CONCLUSIONS

High crystalline and continuous anatase and rutile nano-coatings have been successfully prepared using spray pyrolysis technique. High-temperature stable anatase TiO_2 thin films with $\sim 33\text{nm}$ sized-crystallites have been synthesized using a simple and cost-effective CVD-like process under high-pressure oxygen-enriched atmosphere.

These films constitute promising materials used in hydroxyapatite coated metal implants, rechargeable lithium ion batteries, gas sensors and photocatalytic solar panels.

CONFLICT OF INTEREST

The authors have no conflicts of interest to declare.

REFERENCES

- Ali, B., Rumaiz, A. K., Ozbay, A., Nowak, E. R., & Ismat Shah, S. (2009). Influence of oxygen partial pressure on structural, transport and magnetic properties of Co doped films. *Solid State Communications*, *149* (47-48), 2210-2214. <https://doi.org/10.1016/j.ssc.2009.09.011>
- Aminirastabi, H., Weng, Z., Xiong, Z., Ji, G., & Xue, H. (2017). Evaluation Feature of Nano Grain Growth of TiO₂ Thin Film via Sol-Gel Route. In *Materials Processing Fundamentals 2017* (pp. 33-43). Springer, Cham. https://doi.org/10.1007/978-3-319-51580-9_4
- Bai, Y., Yan, D., Yu, C., Cao, L., Wang, C., Zhang, J., ... Lu, J. (2016). Core-shell Si@ TiO₂ nanosphere anode by atomic layer deposition for Li-ion batteries. *Journal of Power Sources*, *308*, 75-82.
- Ben Jemaa, I., Chaabouni, F., & Abaab, M. (2017). Investigation into the optoelectrical properties of TiO₂ thin films, deposited by RF magnetron sputtering using powder target. *Physica Status Solidi (A)*, *214*(2). <https://doi.org/10.1002/pssa.201600426>
- Castañeda, L., Alonso, J. C., Ortiz, A., Andrade, E., Saniger, J. M., & Bañuelos, J. G. (2003). Spray pyrolysis deposition and characterization of titanium oxide thin films. *Materials Chemistry and Physics*, *77*(3), 938-944. [https://doi.org/10.1016/S0254-0584\(02\)00193-1](https://doi.org/10.1016/S0254-0584(02)00193-1)
- Chandrashekhara, H.D., Angadi, B., Ravikiran, Y.T., Poornima, P., Shashidhar, R., Murthy, L.C.S (2016). Nano porous Al₂O₃-TiO₂ thin film based humidity sensor prepared by spray pyrolysis technique. *AIP Conference Proceedings*, *1728*(1), 020615. DOI: [10.1063/1.4946666](https://doi.org/10.1063/1.4946666)
- Chandrashekhara, H. D., Angadi, B., Shashidhar, R., Murthy, L. C. S., & Poornima, P. (2016). Isochronal Effect of Optical Studies of TiO₂ Thin Films Deposited by Spray Pyrolysis Technique. *Advanced Science Letters*, *22*(4), 739-744. DOI: [10.1166/asl.2016.6975](https://doi.org/10.1166/asl.2016.6975)
- Chen, X., & Mao, S. S. (2007). Titanium dioxide nanomaterials: synthesis, properties, modifications, and applications. *Chemical Reviews*, *107*(7), 2891-2959.
- Choudhury, B., & Choudhury, A. (2013). Local structure modification and phase transformation of TiO₂ nanoparticles initiated by oxygen defects, grain size, and annealing temperature. *International Nano Letters*, *3*(1), 55. <https://link.springer.com/article/10.1186/2228-5326-3-55>
- Chourashiya, M. G. (2013). Studies on synthesis and characterizations of gadolinium doped ceria solid electrolyte. *Self Submission*. Retrieved from <http://shodhganga.inflibnet.ac.in:8080/jspui/handle/10603/9436>
- Deng, D., Kim, M. G., Lee, J. Y., & Cho, J. (2009). Green energy storage materials: Nanostructured TiO₂ and Sn-based anodes for lithium-ion batteries. *Energy & Environmental Science*, *2*(8), 818-837. DOI: [10.1039/b823474d](https://doi.org/10.1039/b823474d)
- Dhandayuthapani, T., Sivakumar, R., & Ilangovan, R. (2016). Single step synthesis of rutile TiO₂ nanoflower array film by chemical bath deposition method. *AIP Conference Proceedings*, *1728*(1), 020286. <https://doi.org/10.1063/1.4946337>
- Dominguez, M. A., & Orduña-Díaz, A. (2017). Fully solution-processed zinc oxide MIS capacitors by ultrasonic spray pyrolysis in air ambient. *Journal of Applied Research and Technology*, *15*(3), 278-282. <https://doi.org/10.1016/j.jart.2017.01.015>
- El, M. K., Brohan, L., Gautier, N., Béchu, S., David, C., Lemaitre, N. & Richard-Plouet, M. (2017). TiO₂ Anatase Solutions for Electron Transporting Layers in Organic Photovoltaic Cells. *Chemphyschem: a European journal of chemical physics and physical chemistry*, *18*(17), 2390-2396. <https://doi.org/10.1002/cphc.201700306>
- Etacheri, V., Seery, M. K., Hinder, S. J., & Pillai, S. C. (2011). Oxygen Rich Titania: A Dopant Free, High Temperature Stable, and Visible-Light Active Anatase Photocatalyst. *Advanced Functional Materials*, *21*(19), 3744-3752. <https://doi.org/10.1002/adfm.201100301>
- Filipovic, L., Selberherr, S., Mutinati, G. C., Brunet, E., Steinhauer, S., Kock, A. & Gspan, C. (2013). Modeling the growth of thin SnO₂ films using spray pyrolysis deposition. *IEEE. International Conference on Simulation of Semiconductor Processes and Devices (SISPAD)*, pp. 208-211.
- Giordano, F., Abate, A., Baena, J. P. C., Saliba, M., Matsui, T., Im, S. H., Graetzel, M. (2016). Enhanced electronic properties in mesoporous TiO₂ via lithium doping for high-efficiency perovskite solar cells. *Nature Communications*, *7*, 10379. <https://doi.org/10.1038/ncomms10379>
- Govindasamy, G., Murugasen, P., Sagadevan, S. (2016). Investigations on the Synthesis, Optical and Electrical Properties of TiO₂ Thin Films by Chemical Bath Deposition (CBD) method. *Materials Research*, *19*(2), 413-419. <https://doi.org/10.1590/1980-5373-MR-2015-0411>
- Hanaor, D. A. H., & Sorrell, C. C. (2011). Review of the anatase to rutile phase transformation. *Journal of Materials Science*, *46*(4), 855-874. <https://link.springer.com/article/10.1007%2Fs10853-0105113-0>
- Jameel, D. A. (2015). Thin film deposition processes. *Thin film deposition processes. International Journal of Modern Physics and Applications*, *1*(4), 193-199.
- Li, H., Martha, S. K., Unocic, R. R., Luo, H., Dai, S., & Qu, J. (2012). High cyclability of ionic liquid-produced TiO₂ nanotube arrays as an anode material for lithium-ion batteries. *Journal of Power Sources*, *218*, 88-92. <https://doi.org/10.1016/j.jpowsour.2012.06.096>
- Li, W., Wang, F., Liu, Y., Wang, J., Yang, J., Zhang, L., ... Zhao, D. (2015). General Strategy to Synthesize Uniform Mesoporous TiO₂/Graphene/Mesoporous TiO₂ Sandwich-Like Nanosheets for Highly Reversible Lithium Storage. *Nano Letters*, *15*(3), 2186-2193. <https://doi.org/10.1021/acs.nanolett.5b00291>
- Lv, L., Chen, Q., Liu, X., Wang, M., & Meng, X. (2015a). Facile synthesis of high-temperature (1000 °C) phase-stable rice-like anatase TiO₂ nanocrystals. *Journal of Nanoparticle Research*, *17*(5), 1-10. <https://doi.org/10.1007/s11051-015-3028-z>
- Lv, L., Chen, Q., Liu, X., Wang, M., & Meng, X. (2015b). Facile synthesis of high-temperature (1000 °C) phase-stable rice-like anatase TiO₂ nanocrystals. *Journal of Nanoparticle Research*, *17*(5), 1-10. <https://doi.org/10.1007/s11051-015-3028-z>
- Lv, L., Li, K., Xie, Y., Cao, Y., & Zheng, X. (2017). Enhanced osteogenic activity of anatase TiO₂ film: Surface hydroxyl groups induce conformational changes in fibronectin. *Materials Science and Engineering: C*, *78*, 96-104. <https://doi.org/10.1016/j.msec.2017.04.056>
- Lv, Y., Yu, L., Huang, H., Liu, H., & Feng, Y. (2009). Preparation, characterization of P-doped TiO₂ nanoparticles and their excellent photocatalytic properties under the solar light irradiation. *Journal of Alloys and Compounds*, *488*(1), 314-319. <https://doi.org/10.1016/j.jallcom.2009.08.116>

- Na, K. J., & Park, G.-C. (2016). Improved Treatment of Photothermal Cancer by Coating TiO₂ on Porous Silicon. *Journal of Nanoscience and Nanotechnology*, 16(2), 1375–1378. <https://doi.org/10.1166/jnn.2016.12024>
- Nakaruk, A., Ragazzon, D., & Sorrell, C. C. (2010). Anatase–rutile transformation through high-temperature annealing of titania films produced by ultrasonic spray pyrolysis. *Thin Solid Films*, 518(14), 3735–3742. <https://doi.org/10.1016/j.tsf.2009.10.109>
- Nakaruk, A., & Sorrell, C. C. (2010). Conceptual model for spray pyrolysis mechanism: fabrication and annealing of titania thin films. *Journal of Coatings Technology and Research*, 7(5), 665–676. <https://doi.org/10.1007/s11998-010-9245-6>
- Oja, I., Mere, A., Krunks, M., Solterbeck, C.-H., & Es-Souni, M. (2004). Properties of TiO₂ Films Prepared by the Spray Pyrolysis Method. *Solid State Phenomena*, 99–100, 259–264. <https://doi.org/10.4028/www.scientific.net/SSP.99-100.259>
- Park, J. Y., Kim, H., Rana, D., Jamwal, D., & Katoch, A. (2017). Surface-area-controlled synthesis of porous TiO₂ thin films for gas-sensing applications. *Nanotechnology*, 28(9), 095502. DOI: 10.1088/1361-6528/aa5836
- Parveen, B., Mahmood-ul-Hassan, Khalid, Z., Riaz, S., & Naseem, S. (2017). Room-temperature ferromagnetism in Ni-doped TiO₂ diluted magnetic semiconductor thin films. *Journal of Applied Research and Technology*, 15(2), 132–139. <https://doi.org/10.1016/j.jart.2017.01.009>
- Periyat, P., Naufal, B., & Ullattil, S. G. (2016). A Review on High Temperature Stable Anatase TiO₂ Photocatalysts. *Materials Science Forum*, 855, 78–93.
- Piercy, B. D., Leng, C. Z., & Losego, M. D. (2017). Variation in the density, optical polarizabilities, and crystallinity of TiO₂ thin films deposited via atomic layer deposition from 38 to 150 °C using the titanium tetrachloride–water reaction. *Journal of Vacuum Science & Technology A: Vacuum, Surfaces, and Films*, 35(3), 03E107. <https://doi.org/10.1116/1.4979047>
- Pillai, S. C., Periyat, P., George, R., McCormack, D. E., Seery, M. K., Hayden, H., Hinder, S. J. (2007). Synthesis of high-temperature stable anatase TiO₂ photocatalyst. *The Journal of Physical Chemistry C*, 111(4), 1605–1611.
- Rahim, M. S., Sahdan, M. Z., Bakri, A. S., Yunus, S. H. A., & Lias, J. (2016). Low Temperature Growth of High Quality Crystal of Anatase Based-TiO₂ Thin Film Grown Using Double Zone CVD Technique. In *2016 World Symposium on Computer Applications Research (WSCAR)* (pp. 126–129). <https://doi.org/10.1109/WSCAR.2016.23>
- Shinde, P. S. (2012). Photoelectrochemical Detoxification of water using spray deposited oxide semiconductor thin films. INFLIBNET. Retrieved from <http://shodhganga.inflibnet.ac.in:8080/jspui/handle/10603/139462>
- Singh, J., Sahu, K., Kuriakose, S., Tripathi, N., Avasthi, D. K., & Mohapatra, S. (2017). Synthesis of nanostructured TiO₂ thin films with highly enhanced photocatalytic activity by atom beam sputtering. *Adv Mater Lett*, 8, 107–113.
- Song, Z. (2016). *Solution Processed High Efficiency Thin Film Solar Cells: from Copper Indium Chalcogenides to Methylammonium Lead Halides*. University of Toledo. Retrieved from https://etd.ohiolink.edu/pg_10?0::NO:10:P10_ACCESSION_NUM:toledo1470403462
- Uchida, M., Kim, H.-M., Kokubo, T., Fujibayashi, S., & Nakamura, T. (2003). Structural dependence of apatite formation on titania gels in a simulated body fluid. *Journal of Biomedical Materials Research. Part A*, 64(1), 164–170. <https://doi.org/10.1002/jbm.a.10414>
- Vodišek, N., Ramanujachary, K., Brezová, V., & Lavrenčič Štangar, U. (2017). Transparent titania-zirconia-silica thin films for self-cleaning and photocatalytic applications. *Catalysis Today*, 287, 142–147. <https://doi.org/10.1016/j.cattod.2016.12.026>
- Wang, Z., Zhong, Z., McKeown Walker, S., Ristic, Z., Ma, J.-Z., Bruno, F. Y., Radovic, M. (2017). Atomically Precise Lateral Modulation of a Two-Dimensional Electron Liquid in Anatase TiO₂ Thin Films. *Nano Letters*, 17(4), 2561–2567. <https://doi.org/10.1021/acs.nanolett.7b00317>
- Xia, W., Lindahl, C., Lausmaa, J., & Engqvist, H. (2011). Biomimetic Hydroxyapatite Deposition on Titanium Oxide Surfaces for Biomedical Application. In A. George (Ed.), *Advances in Biomimetics*. InTech. Retrieved from <http://www.intechopen.com/books/advances-in-biomimetics/biomimetic-hydroxyapatite-deposition-on-titanium-oxide-surfaces-for-biomedical-application>
- You, H. C. (2015). Transistor Characteristics of Zinc Oxide Active Layers at Various Zinc Acetate Dihydrate Solution Concentrations of Zinc Oxide Thin-film. *Journal of Applied Research and Technology*, 13(2), 291–296. <https://doi.org/10.1016/j.jart.2015.06.003>
- Ziegler, J., Yang, F., Wagner, S., Kaiser, B., Jaegermann, W., Urbain, F., Finger, F. (2016). Interface engineering of titanium oxide protected a-Si:H/a-Si:H photoelectrodes for light induced water splitting. *Applied Surface Science*, 389, 73–79. <https://doi.org/10.1016/j.apsusc.2016.07.074>